Synthesis, characterization, DFT calculations and antimicrobial activity of Pd(II) and Co(III) complexes with the condensation derivative of 2-(diphenylphosphino)benzaldehyde and Girard's T reagent

Kawther Adaila[a], Milica Milenković[a], Alessia Bacchi[b], Giulia Cantoni[b], Marcel Swart[cd], Maja Gruden-Pavlović[a], Marina Milenković[e], Božidar Čobeljić[a], Tamara Todorović[a] & Katarina Anđelković[a]

[a] Faculty of Chemistry, University of Belgrade, Studentski trg 12-16, 11000 Belgrade, Serbia

[b] Dipartimento di Chimica Generale ed Inorganica, Chimica Analitica, Chimica Fisica, University of Parma, Parco Area delle Scienze 17 A, I 43100 Parma, Italy

[c] Institució Catalana de Recerca i Estudis Avançats (ICREA), Pg. Lluís Companys 23, 08010 Barcelona, Spain

[d] Institut de Química Computacional i Catàlisi and Departament de Química, Universitat de Girona, Campus Montilivi, 17071 Girona, Spain

[e] Department of Microbiology and Immunology, Faculty of Pharmacy, University of Belgrade, Vojvode Stepe 450, Serbia
Accepted author version posted online: 03 Oct 2014.

PLEASE SCROLL DOWN FOR ARTICLE

Synthesis, characterization, DFT calculations and antimicrobial activity of Pd(II) and Co(III) complexes with the condensation derivative of 2-(diphenylphosphino)benzaldehyde and Girard's T reagent

KAWTHER ADAILA[a], MILICA MILENKOVIĆ[a], ALESSIA BACCHI[b], GIULIA CANTONI[b], MARCEL SWART[c,d], MAJA GRUDEN-PAVLOVIĆ[a], MARINA MILENKOVIĆ[e], BOŽIDAR ČOBELJIĆ[a], TAMARA TODOROVIĆ[a] and KATARINA ANĐELKOVIĆ1[a]

[a]Faculty of Chemistry, University of Belgrade, Studentski trg 12–16, 11000 Belgrade, Serbia
[b]Dipartimento di Chimica Generale ed Inorganica, Chimica Analitica, Chimica Fisica, University of Parma, Parco Area delle Scienze 17 A, I 43100 Parma, Italy
[c]Institució Catalana de Recerca i Estudis Avançats (ICREA), Pg. Lluís Companys 23, 08010 Barcelona, Spain
[d]Institut de Química Computacional i Catàlisi and Departament de Química, Universitat de Girona, Campus Montilivi, 17071 Girona, Spain
[e]Department of Microbiology and Immunology, Faculty of Pharmacy, University of Belgrade, Vojvode Stepe 450, Serbia

Complexes of Pd(II) and Co(III) with the condensation derivative of 2-(diphenylphosphino)benzaldehyde and Girard T reagent were synthesized, characterized, and their antimicrobial activities were evaluated. The ligand and the complexes were characterized by elemental analysis, IR and NMR spectroscopy and X-ray crystallography. In both complexes, the deprotonated ligand was coordinated to the metal through the phosphorus, the imine nitrogen and the carbonyl oxygen atoms. In the octahedral Co(III) complex two molecules of ligands were coordinated to metal ion, while square-planar environment of Pd(II) complex was constituted of one tridentate ligand and chloride in the fourth coordination place. The ligand and complexes showed moderate antibacterial activity. The molecular structures of the obtained metal complexes and the relative stabilities of two stereoisomers of the ligand were calculated using DFT at the S12g/TZ2P level.

Keywords: Pd(II) complex; Co(III) complex; Derivative of 2-(diphenylphosphino)benzaldehyde; X-ray structure; DFT calculations

1. Introduction

1Corresponding author. Email: kka@chem.bg.ac.rs

Hydrazone derivatives of 2-(diphenylphosphino)benzaldehyde and corresponding metal complexes have been intensively investigated because of their theoretical importance [1], application in analytical chemistry [2] and possible catalytic [3] and biological activity [4]. Our research in this area has been directed on synthesis, structure characterization and biological activity examination of different 2-(diphenylphosphino)benzaldehyde hydrazones and corresponding transition metal complexes in order to establish a possible relationship between their structure and biological activity. At the beginning of our study, we synthesized condensation product of 2-(diphenylphosphino)benzaldehyde and semioxamazide and its Pd(II), Pt(II) and Ni(II) complexes. In these complexes, the monodeprotonated ligand was coordinated tridentate through phosphorus, imine nitrogen and carbonyl oxygen atoms generating five-membered and six-membered chelation rings, while the fourth coordination place occupied by chloride ligand in the complexes of Pd(II) and Pt(II) or cyanate anion in Ni(II) complex. Complexes of Pd(II) and Pt(II) adopted square planar geometry, whereas the geometry of the Ni(II) complex was tetrahedral. The antimicrobial activity of ligand and complexes was of the same order of magnitude as standard antibiotic and antifungal agents [5]. The cytotoxic activity of Pd(II) and Pt(II) complexes was similar to that of cisplatin [6]. The research was continued with the synthesis of 2-(diphenylphosphino)benzaldehyde and ethyl hydrazinoacetate and corresponding Pd(II) complex. In square-planar Pd(II) complex, the ligand was coordinated through phosphorus and imine nitrogen atoms forming one six-membered chelate ring, while third and fourth coordination places were occupied by chloride ligands. Complex of Pd(II) has a similar effect to cisplatin, inducing apoptosis and cell cycle perturbation [6]. From the reaction of 2-(diphenylphosphino)benzaldehyde and ethyl carbazate we obtained ligand which differs from previously synthesized condensation product of 2-(diphenylphosphino)benzaldehyde and ethyl hydrazinoacetate in only one methylene group between hydrazine nitrogen and carbonyl oxygen atoms [7]. This modification allows tridentate coordination of ligand via phosphorus, imine nitrogen and carbonyl oxygen atoms with formation of six-membered and five-membered chelation rings. We described the synthesis, characterization and biological activity evaluation of octahedral Co(III) [7] and Fe(III) complexes [8], as well as square-planar Pd(II) [8] and Ni(II) complexes [9] with the condensation derivative of 2-(diphenylphosphino)benzaldehyde and ethyl carbazate. In both octahedral complexes, coordination surroundings around metal ion consist of two tridentate PNO coordinated ligands, while in square-planar complexes one deprotonated

2

ligand is PNO coordinated to metal and the fourth coordination place was occupied by chloride anion in the case of Pd(II) complex or monodentate pseudohalides (cyanate, thiocyanate or azide) in Ni(II) complexes [7-9]. Complex of Co(III) exhibited strong cytotoxic activity, stronger than cisplatin [7]. The Ni(II) complexes showed cytotoxic activity to all tested tumor cell lines with the most pronounced to leukemia cell line K562. The complexes influenced the cell cycle of tumor cells and induced plasmid DNA cleavage. The biological activity of Ni(II) complexes depends on the nature of monodentate pseudohalide ligand [9]. It was observed that antimicrobial activity of complexes of Co(III), Fe(III), Pd(II) and Ni(II) depends on geometry and charge of complex particles. Electrolyte complexes of Co(III) and Fe(III) with octahedral geometry have a more pronounced antibacterial activity, while the square-planar non-electrolyte complexes of Pd(II) and Ni(II) were found to be better antifungal agents [7-9].

In this manuscript, the synthesis, the characterization and the biological activity of condensation product of 2-(diphenylphosphino)benzaldehyde and Girard's T reagent and its Co(III) and Pd(II) complexes were described. The aim of this study was to investigate the influence of enhanced hydrophilicity of charged tridentate PNO hydrazone ligand on biological activity.

2. Experimental

2.1. *Materials*

2-(Diphenylphosphino)benzaldehyde (97%) and Girard's T reagent (99%) were obtained from Aldrich. Ethanol and methanol were reagent grade and used without purification.

2.2. *Synthesis of (E)-2-(2-(2-(diphenylphosphino)benzylidene)hydrazinyl)-N,N,N-trimethyl-2-oxoethan-1-aminium chloride monoethanole* (HL·EtOH)

A mixture of 140 mg (0.48 mmol) 2-(diphenylphosphino)benzaldehyde and 80 mg (0.48 mmol) Girard's T reagent was dissolved, by heating, in 20 mL ethanol and one drop of concentrated hydrochloric acid was added. The mixture was refluxed for 60 min. The reaction solution was left to stand at room temperature while the colorless crystals separated from the solution. Yield: 110 mg (47%); Mp 216 °C. IR (vs-very strong, s-strong, m-medium, w-weak): 3524 (w), 3403 (w), 3308 (w), 3050 (m), 3018 (m), 2970 (m), 2930 (m), 2890 (m), 2817 (w), 1686 (vs), 1657 (m), 1602 (w), 1491 (w), 1475 (s), 1433 (s), 1410 (s), 1342 (w), 1306 (s), 1277 (w),

3

1212 (w), 1133 (w), 1123 (m), 1095 (w), 1044 (w), 992 (w), 948 (w), 929 (w), 876 (w), 848 (w), 765 (w), 746 (vs), 699 (s), 620 (w), 585 (w), 505 (w), 481 (w), 437 (w). Anal. Calcd. for $C_{24}H_{27}ClN_3O_2P \cdot EtOH$ (%): N, 8.65; C, 64.26; H, 6.84. Found: N, 8.78; C, 64.17; H, 6.92.

2.3. *Synthesis of Pd(II) complex* (1)

The ligand (80 mg (0.16 mmol) was dissolved, by heating at 65 °C, in 35 mL H_2O. After that, a solution of $K_2[PdCl_4]$, prepared by dissolving 60 mg (0.18 mmol) in 5 mL H_2O, was added to it. Right after that, the mixing temperature was decreased to 52 °C and the mixture was kept at that temperature for 1 h. The reaction solution was evaporated under vacuum, dissolved in 10 mL of methanol and the solution was filtered. After two days yellow crystals of Pd(II) complex arose from methanolic solution. Yield: 30 mg (32%). IR (vs-very strong, s-strong, m-medium, w-weak): 3391 (m), 3053 (w), 3010 (w), 2959 (w), 1639 (m), 1547 (s), 1484 (m), 1436 (m), 1398 (w), 1369 (w), 1343 (w), 1315 (w), 1275 (w), 1213 (w), 1180 (w), 1139 (w), 1101 (w), 1028 (w), 997 (w), 975 (w), 933 (w), 912 (w), 868 (w), 807 (w), 772 (w), 748 (w), 691 (m), 588 (w), 547 (w). Anal. Calcd. for $C_{24}H_{26}Cl_2N_3OPPd$ (%): N, 7.23; C, 49.63; H, 4.51. Found: N, 7.36; C, 49.74; H, 4.46.

2.4. *Synthesis of Co(III) complex* (2)

The ligand (140 mg, 0.29 mmol) was dissolved, by heating, in $EtOH/H_2O$ mixture (10 mL/10 mL) and solid $Co(BF_4)_2 \cdot 6H_2O$ (100 mg, 0.29 mmol) was added. The reaction mixture was heated at 65 °C for 4 h. The color of the solution changed to red. The reaction solution was left to stand at room temperature, while red crystals precipitated from solution. Yield: 50 mg (29%). IR (vs-very strong, s-strong, m-medium, w-weak): 3599 (m), 3559 (m), 3473 (w), 3060 (w), 2995 (w), 1619 (w), 1572 (m), 1483 (m), 1436 (m), 1412 (w), 1322 (m), 1222 (w), 1058 (vs), 926 (m), 872 (w), 753 (m), 698 (m), 593 (w), 525 (m), 495(w). Anal. Calcd. for $C_{48}H_{52}B_3CoF_{12}N_6O_2P_2 \cdot 3H_2O$ (%): N, 7.12; C, 48.84; H, 4.95. Found: N, 7.03; C, 48.86; H, 5.04.

2.5. *Physical measurements*

IR spectra were recorded on a Perkin–Elmer FT-IR 1725X spectrometer using the ATR technique in the region 4000−400 cm^{-1}. ^1H-NMR (500 MHz), ^{13}C-NMR (125 MHz) and 2D-NMR spectra were recorded on a Bruker Avance 500 spectrometer in DMSO–d^6 using TMS

4

as internal standard for ^{1}H and ^{13}C. All spectra were measured at room temperature. Elemental analyses (C, H and N) were performed by standard micro-methods using the ELEMENTARVario ELIII C.H.N.S.O analyzer.

2.6. *X-ray analysis of* **HL·EtOH,** **1** *and* **2**

Single crystal X-ray diffraction data were collected using the Mo Kα radiation ($\lambda = 0.71073$ Å) at T = 293 K on a SMART diffractometer with Breeze area detector. The collected intensities were corrected for Lorentz and polarization factors and empirically for absorption by using the SADABS program [10]. Structures were solved by direct methods using SIR2011 [11] and refined by full-matrix least-squares on all F^2 using SHELXL97 [12] implemented in the Olex2 package [13]. Hydrogens were introduced in calculated positions. Anisotropic displacement parameters were refined for all non-hydrogen atoms. Hydrogen bonds have been analyzed with SHELXL97 [12] and PARST97 [14] and extensive use was made of the Cambridge Crystallographic Data Centre packages [15] for the analysis of crystal packing. Compound **2** presented problematic data, with a very large unit cell containing many disordered anions and possibly solvent molecules that have not been located in the electron density map. Three independent cations are clearly determined, but they present high thermal mobility and therefore also contribute to poor data quality. The molecular structure of the cations has been restrained, especially for the trimethylammonium moieties that were not totally visible in the electron density maps. The final structure demonstrates the molecular connectivity, but no further discussion is attempted. Crystals of **1** were radiation sensitive and data were corrected for decay. The structure is made by an ordered and stable part consisting of complex cations and anions and refines very well, and by an unknown disordered part contained in channels (Supplementary Material). The final structure has been optimized by accounting for disordered density by the masking procedure implemented in Olex2. It was not possible to determine the nature of the disordered content of the crystal. Table 1 summarizes crystal data and structure determination results for **HL·EtOH** and **1**, while results for **2** are in the Supplementary Material. Crystallographic data (excluding structure factors) for **HL·EtOH**, **1** and **2** have been deposited with the Cambridge Crystallographic Data Centre as supplementary publications nos. CCDC 1013634 (**HL·EtOH**), 1013635 (**2**) and 1013636 (**1**). Copies of the data can be obtained free of

charge on application to CCDC, 12 Union Road, Cambridge CB2 1EZ, UK (Fax: (+44) 1223-336-033; E-mail: deposit@ccdc.cam.ac.uk).

2.7. *DFT computational details*

The calculations using the restricted Kohn–Sham formalism have been performed with the Amsterdam Density Functional (ADF) program package, version 2013.01 [16] with generalized gradient approximation functional S12g [17] which includes Grimme's D_3 dispersion energy [18]. A basis set of triple-zeta Slater-type orbitals (STO) plus two polarization functions (TZ2P) with a small frozen core has been used for all atoms. Due to the presence of cobalt and palladium, scalar relativistic corrections have been included self-consistently by using the zeroth-order regular approximation (ZORA) [19]. The conductor like screening solvation model (COSMO) [20], as implemented in ADF [21], was included in the density functional theory (DFT) geometry optimizations with water as a solvent [22]. Analytical harmonic frequencies [23] were calculated and in all cases the global minimum was confirmed by the absence of imaginary frequency modes.

2.8. *Antimicrobial activity*

The antimicrobial activity was investigated on six different laboratory control strains of bacteria, *i.e.*, the Gram-positive: *Staphylococcus aureus* (ATCC 6538), *Bacillus subtilis* (ATCC 6633) and the Gram-negative: *Escherichia coli* (ATCC 10536), *Klebsiella pneumoniae* (NCIMB 9111), *Pseudomonas aeruginosa* (ATCC 9027), *Salmonella abony* (NCTC 6017) and one strain of yeast, *i.e.*, *Candida albicans* (ATCC 10231). All tests were performed in Müller Hinton broth for the bacterial strains and in Sabouraud dextrose broth for the yeast. Overnight broth cultures of each strain were prepared, and the final concentration in each well was adjusted to $2 \cdot 10^6$ CFU/mL for the bacteria and $2 \cdot 10^5$ CFU/mL for the yeast. **HL·EtOH**, **1** and **2** were dissolved in 1% dimethylsulfoxide (DMSO) and then diluted to the highest concentration. Twofold serial concentrations of the compounds were prepared in a 96-well microtiter plate over the concentration range 62.5–1000 μgL^{-1}. The microbial growth was determined after 24 h incubation at 37 °C for the bacteria and after 48 h incubation at 26 °C for the fungi. The MIC is defined as the lowest concentration compound at which no visible growth of microorganism is observed.

6

3. Results and discussion

3.1. *General*

The condensation reaction of the Girard's T reagent with 2-(diphenylphosphino)benzaldehyde results in the formation of the corresponding hydrazone as an ammonium quaternary chloride salt. Complex of Pd(II) (**1**) was prepared by substitution reaction starting from $K_2[PdCl_4]$ and the ligand (**HL·EtOH**) (scheme 1a). Complex of Co(III) (**2**) was obtained by direct synthesis in the reaction of **HL·EtOH** and $Co(BF_4)_2 \cdot 6H_2O$ (scheme 1b).

3.2. *IR spectra*

In the IR spectrum of **HL·EtOH** there is a band at 1657 cm^{-1} originating from the azomethine group (v(C=N)) [1f]. Instead of the carbonyl band from the uncoordinated ligand at 1686 cm^{-1}, in the IR spectra of complexes a new band appeared at 1619 cm^{-1} in the spectrum of Co(III) complex (**2**) and at 1639 cm^{-1} in the spectrum of Pd(II) complex (**1**) corresponding to v($^-$O−C=N) of the deprotonated hydrazide moiety [5]. The band at 1657 cm^{-1} originating from the azomethine group [v(C=N)] from the uncoordinated ligand shifted to 1572 cm^{-1} in the spectrum of **2**, while in the spectrum of **1** this band appeared at 1547 cm^{-1}, indicating that imine nitrogen was involved in coordination. The position of the band attributed to v(C−P) vibrations is almost constant in the IR spectra of ligand and the complexes (1433 cm^{-1} in the spectrum of ligand, 1436 cm^{-1} in spectra of both of the complexes) [5]. The band originating from the tetrafluoroborate anions in the outer sphere of the Co(III) complex is at 1058 cm^{-1} [7, 24].

3.3. *NMR spectra*

Hydrazone can exist as different isomers, due to geometric isomerism related to the imino group (*E, Z* isomers) and rotational isomerism as a result of restricted rotation around amide bound (*anti, syn* conformers) [25]. Results of X-ray analysis of ligand demonstrated that reaction of 2-(diphenylphosphino)benzaldehyde with the Girard's T reagent results in the formation of its *E* isomer. NMR data for ligand revealed the presence of two stereoisomers *syn* and *anti* in solution.

    The ^{1}H NMR spectrum of ligand showed two singlet signals of hydrazide NH at 12.10 ppm and 12.70 ppm [4], corresponding to *syn* and *anti* isomers, respectively [26]. Two singlets were observed for azomethine group at 8.79 ppm and 9.02 ppm, corresponding to *syn*

7

and *anti* isomers, respectively [5, 26]. Also, double signals were noticed for methyl, methylene and aromatic hydrogen atoms H5 and H8. The aromatic protons appeared in the region from 6.83 to 8.05 ppm. Based on integral of hydrogen atom signals the ratio of *syn/anti* isomer of ligand is 0.75:0.25. The signal of hydrazide NH in the spectra of both complexes is missing, indicating that the ligand is coordinated in deprotonated form [4]. Coordination through imine nitrogen results in downfield shift of H3 in **2** [7], while in **1** this signal was shifted upfield [4, 8]. In the ^{1}H NMR spectra of complexes signals of most aromatic protons shift downfield, suggesting that coordination occurs through phosphorus (table 2).

In ^{13}C NMR spectrum of **HL·EtOH** double signals of *syn* and *anti* isomers are also observed (table 3). The ^{13}C NMR spectrum showed two signals for carbonyl group at 165.5 and 160.1 ppm, and two signals for azomethine group at 143.4 and 146.5 ppm corresponding to *syn* and *anti* isomers, respectively. Coordination through carbonyl oxygen atom results in downfield shift of its signal in the spectra of complexes (170.0 ppm in the spectrum of **1** and 168.8 ppm in the spectrum of **2**) [4, 7, 8]. The signal of imine C3 is shifted downfield in the spectra of complexes due to coordination through imine nitrogen (154.0 ppm in the spectrum of **1** and 165.2 ppm in the spectrum of **2**) [4]. In **1**, signals of aromatic carbon atoms directly bound to phosphorus shift upfield due to coordination through phosphorus [7]. In both complexes, the chemical shifts of most aromatic carbon atoms have higher values, due to electron withdrawal by the coordinated metal ion.

3.4. *Description of crystal structure*

Compound **HL·EtOH** crystallizes as a quaternary ammonium chloride salt, protonated on the amidic nitrogen and with a chloride counter-anion to balance the total charge, forming a hydrogen bond between these two groups (NH…Cl = 3.264(2) Å, 164(1)°) (figure 1). The ligand skeleton is skewed, with torsion angles: C3–C18–C19–N1 = 158°, C18–C19–N1–N2 = 176°, C19–N1–N2–C20 = 177°, N1–N2–C20–C21 = –105°. An ethanol molecule completes the asymmetric unit and forms a hydrogen bond with the chloride anion (O–H…Cl = 3.129(3) Å, 179(1)°).

Compound **1** crystallizes with two independent cationic complexes in the asymmetric unit (figure 2), that are not significantly different, and are related by a pseudo twofold rotation axis, not aligned with the cell edges (see Supplementary Material). The unit cell is completed by

8

two chlorides, one of which distributed over two positions on inversion centers. Both complex molecules [Pd**L**Cl]$^+$ (figure 2) present a square planar coordination around the metal atom, made by the PNO tridentate neutral zwitterionic ligand and completed by a chloride *trans* to the N atom. Table 4 reports the most relevant bond distances and angles. The phosphorus atom is slightly displaced from the coordination plane, as usually observed for similar families of PNO ligands [1(e)]. Upon coordination of the tridentate ligand, five-membered and six-membered chelation rings are formed, the former planar, the latter slightly puckered due to the above mentioned hindrance of the phosphorus atom. The trimethylamino cationic tail of the ligand is oriented almost perpendicular to the ligand plane. Interestingly, the two complex cations are stacked with the coordination planes parallel with a Pd...Pd distance of 4.313 Å (figure 2, inset), forming other short contacts between the aromatic CH and the chlorides and between the CH$_2$ groups and the iminic N atoms. The chlorides are nested between the methyl groups of the cationic tail of the complex molecules, so that in the overall packing (figure 3) the moieties with different polarity are compartmentalized in a slice of phenyl groups, a slice of stacked coordination planes, and a slice of trimethylammonium moieties alternating with chloride anions. This organization leaves large voids in the crystal that are occupied by disordered solvent ready to leave the solid and to decompose upon X-ray exposure. It has not been possible to build a sensible chemical model for this contribution, whose overall electron density is presented in the Supplementary Material.

Compound **2** crystallizes in the space group *Cc* in a huge cell, with a volume of 16841 Å^3 (see Supplementary Material). The asymmetric unit contains three independent cations [Co**L**$_2$]$^{3+}$, and nine BF$_4$$^-$ anions, most of which were not visible in the electron density map. The structure is in fact highly disordered and the quality of diffraction data was not sufficient for an accurate determination of the molecular geometry and crystal packing. The connectivity of the complex cations is unambiguous and is shown in figure 4. The complex has a bis(trischelate) PNO coordination on the metal centre, giving an octahedral geometry, with the formation of five-membered and six-membered chelation rings. The three cations in the asymmetric unit present different *Δ/Λ* absolute configuration on the metal, two being of the same configuration and the third being different; since the space group contains a symmetry plane, the compound is racemic.

9

3.5. *DFT calculations*

Hydrazone can exist as different isomers due to geometric isomerism with respect to the imino group (*E*, *Z* isomers) and rotational isomerism as a result of hindered rotation about the amide linkage (*anti*, *syn* stereoisomers). DFT calculations revealed that the *E* isomers are more stable than the *Z* isomers. The NMR studies of the prepared ligand showed the presence of a mixture of two *syn* and *anti* stereoisomers in solution. The present DFT calculations showed that the *syn E* stereoisomer is slightly more stable than the *anti E* isomer; the energy difference between them does not exceed 0.1 kcal/mol. This very small energy difference indicates their coexistence in equilibrium in the solution, which corroborates the experimental findings.

Since the X-ray determined structures of **1** and **2** were highly disordered, DFT calculations were performed to verify the geometry of the metal complexes. Indeed, DFT calculations confirmed a square-planar geometry for [Pd**L**Cl]$^+$ (more stable in energy than the tetrahedral isomer by 39 kcal/mol) and an octahedral arrangement and singlet ground state for [Co**L**$_2$]$^{3+}$. Furthermore, the calculated results for both complexes match almost perfectly with the experimental data, giving us considerable confidence about the structures of **1** and **2** (figures 5 and 6). The molecular energies and Cartesian coordinates are given in the Supplementary Material.

3.6. *Antimicrobial activity*

Antimicrobial activities of **1** and **2** were higher than the activity of **HL·EtOH** (table 5). Complex **2** exhibited strong activity against Gram-positive bacteria *S. aureus* and Gram-negative bacteria *S. abony*, *P. aeruginosa* and *K. pneumoniae*. A moderate activity of **2** was observed against the other examined bacterial strains. Complex **1** and **HL·EtOH** showed moderate activity on most of the tested bacterial strains. The most pronounced activity of **1** was observed against Gram-negative bacteria *P. aeruginosa* and *S. abony*. The strongest antimicrobial activity of **HL·EtOH** was noted against *S. abony*. **HL·EtOH**, **1** and **2** are not good antifungal agents, among them the highest antifungal activity was observed for **2**.

Comparison of antimicrobial activities of **HL·EtOH**, **1** and **2** with the activity of previously investigated condensation product of 2-(diphenylphosphino)benzaldehyde and ethyl carbazate and corresponding complexes of Pd(II) [8] and Co(III) [7] gives insight into the influence of hydrophobicity, charge and geometry of complexes on biological activity. The

10

highest antibacterial activity was observed for octahedral electrolytic Co(III) complexes, while the best antifungal activity was observed for neutral square planar Pd(II) complex with condensation product of 2-(diphenylphosphino)benzaldehyde and ethyl carbazate. The presence of positively charged ligand in Pd(II) complex results in decreased antifungal activity and better antibacterial activity. An opposite situation was observed in the case of octahedral Co(III) complexes for which better antibacterial activity was observed for complex with uncharged ligand. Complex **1** showed better antimicrobial activity in comparison with previously synthesized Pd(II) complexes with similar PNO donor ligands [4, 5].

4. Conclusion

We present here the synthesis and the structural characterization of (*E*)-2-(2-(2-(diphenylphosphino)benzylidene)hydrazinyl)-*N*,*N*,*N*-trimethyl-2-oxoethan-1-aminium chloride monoethanol (**HL·EtOH**) as well as its Pd(II) and Co(III) complexes. From the condensation reaction of the Girard's T reagent with 2-(diphenylphosphino)benzaldehyde, an ammonium quaternary chloride salt of the ligand was obtained. Square-planar Pd(II) complex is in the cationic form [Pd**L**Cl]$^+$ with the deprotonated ligand coordinated tridentate via the phosphorus, the imine nitrogen and the carbonyl oxygen atoms, and chloride as counter-ion. Co(III) complex consists of cation [Co**L**$_2$]$^{3+}$ counterbalanced by three BF$_4^-$ anions. The Co(III) complex has a bis(trischelate) PNO coordination on the metal centre, giving an octahedral geometry. NMR data for the ligand revealed the presence of *syn* and *anti* stereoisomers in solution, proved by DFT calculations. The structures of the metal complexes with the different coordination spheres were confirmed by the DFT calculations and found to be in excellent agreement with the experimental X-ray results. Antimicrobial activities of **1** and **2** were higher than the activity of **HL·EtOH**. Complex **2** exhibited strong activity against *S. aureus*, *S. abony*, *P. aeruginosa* and *K. pneumoniae*. Complex **1** and ligand showed moderate activity on most of the tested bacterial strains. The most pronounced activity of **1** was observed against *P. aeruginosa* and *S. abony*. Results of antimicrobial activity showed that charge, geometry and nature of metal ion in **1** and **2** have important influence on biological activity. Octahedral Co(III) and square–planar Pd(II) complexes with large variety of ligands were investigated as potential antimicrobial and antitumor agents [27-34], among them complexes with stronger activity than **1** and **2** are reported [32, 33]. Having all these facts in mind, it is obvious that nature of the coordinated ligands have

11

strong effect on solubility, stability, steric, electronic and pharmacokinetic properties of metal complexes as well as on mechanism of their action.

Acknowledgements

References

[1] (a) A. Kobayashi, D. Yamamoto, H. Horiki, K. Sawaguchi, T. Matsumoto, K. Nakajima, H. Chang, M. Kato. *Inorg. Chem.*, **53**, 2573 (2014). (b) P. Pelagatti, A. Bacchi, M. Balordi, A. Caneschi, M. Giannetto, C. Pelizzi, L. Gonsalvi, M. Peruzzini, F. Ugozzoli. *Eur. J. Inorg. Chem.*, **2007**, 162 (2007). (c) P. Pelagatti, A. Bacchi, M. Carcelli, M. Costa, H. Frühauf, K. Goubitz, C. Pelizzi, M. Triclistri, K. Vrieze. *Eur. J. Inorg. Chem.*, **2002**, 439 (2002). (d) P. Pelagatti, A. Bacchi, C. Bobbio, M. Carcelli, M. Costa, A. Fochi, C. Pelizzi. *J. Chem. Soc.*, *Dalton Trans.*, 1820 (2002). (e) A. Bacchi, M. Carcelli, M. Costa, A. Fochi, C. Monici, P. Pelagatti, C. Pelizzi, G. Pelizzi, L.M.S. Roca. *J. Organomet. Chem.*, **593–594**, 180 (2000). (f) A. Barandov, U. Abram. *Z. Anorg. Allg. Chem.*, **633**, 1897 (2007). (g) S.B. Novaković, G.A. Bogdanović, I.D. Brčeski, V.M. Leovac. *Acta Crystallogr. C*, **65**, 263 (2009). (h) V.M. Leovac, B. Ribár, G. Argay, A. Kálmán, I. Brčeski. *J. Coord. Chem.*, **39**, 11 (1996).

[2] H. Li, J. Fan, M. Hu, G. Cheng, D. Zhou, T. Wu, F. Song, S. Sun, C. Duan, X. Peng. *Chem. Eur. J.*, **18**, 12242 (2012).

[3] (a) A. Ros, B. Estepa, A. Bermejo, E. Álvarez, R. Fernández, J.M. Lassaletta. *J. Org. Chem.*, **77**, 4740 (2012). (b) A. Bacchi, M. Carcelli, M. Costa, A. Leporati, E. Leporati,

P. Pelagatti, C. Pelizzi, G. Pelizzi. *J. Organomet. Chem.*, **535**, 107 (1997). (c) P. Pelagatti, A. Bacchi, M. Carcelli, M. Costa, A. Fochi, P. Ghidini, E. Leporati, M. Masi, C. Pelizzi, G. Pelizzi. *J. Organomet. Chem.*, **583**, 94 (1999). (d) P. Pelagatti, A. Bacchi, M. Balordi, S. Bolaño, F. Calbiani, L. Elviri, L. Gonsalvi, C. Pelizzi, M. Peruzzini, D. Rogolino. *Eur. J. Inorg. Chem.*, **2006**, 2422 (2006).

[4]   M.M. Đorđević, D.A. Jeremić, M.V. Rodić, V.S. Simić, I.D. Brčeski, V.M. Leovac. *Polyhedron*, **68**, 234 (2014).

[5]   V. Radulović, A. Bacchi, G. Pelizzi, D. Sladić, I. Brčeski, K. Andjelković. *Monatsh. Chem.*, **137**, 681 (2006).

[6]   N. Malešević, T. Srdić, S. Radulović, D. Sladić, V. Radulović, I. Brčeski, K. Anđelković. *J. Inorg. Biochem.*, **100**, 1811 (2006).

[7]   M. Milenković, A. Bacchi, G. Cantoni, S. Radulović, N. Gligorijević, S. Aranđelović, D. Sladić, M. Vujčić, D. Mitić, K. Anđelković. *Inorg. Chim. Acta*, **395**, 33 (2013).

[8]   M. Milenković, G. Cantoni, A. Bacchi, V. Spasojević, M. Milenković, D. Sladić, N. Krstić, K. Anđelković. *Polyhedron*, **80**, 47 (2014).

[9]   M. Milenković, A. Bacchi, G. Cantoni, J. Vilipić, D. Sladić, M. Vujčić, N. Gligorijević, K. Jovanović, S. Radulović, K. Anđelković. *Eur. J. Med. Chem.*, **68**, 111 (2013).

[10] SAINT: SAX, Area Detector Integration, Siemens Analytical instruments INC., Madison, Wisconsin, USA; SADABS: Siemens Area Detector Absorption Correction Software, G. Sheldrick, University of Gottingen, Germany (1996).

[11] Sir2011: M.C. Burla, R. Caliandro, B. Carrozzini, G.L. Cascarano, C. Giacovazzo, M. Mallamo, A. Mazzone, G. Polidori, Istituto di Ricerca per lo Sviluppo di Metodologie Cristallografiche CNR, Bari (2011).

[12] Shelxl97. Program for structure refinement, G. Sheldrick, University of Gottingen, Germany (1997).

[13] O.V. Dolomanov, L.J. Bourhis, R.J. Gildea, J.A.K. Howard, H. Puschmann. *J. Appl. Cryst.*, **42**, 339 (2009).

[14] M. Nardelli. *J. Appl. Cryst.*, **28**, 659 (1995).

[15] (a) F.H. Allen, O. Kennard, R. Taylor. *Acc. Chem. Res.*, **16**, 146 (1983). (b) I.J. Bruno, J.C. Cole, P.R. Edgington, M. Kessler, C.F. Macrae, P. McCabe, J. Pearson, R. Taylor. *Acta Crystallogr.*, **B58**, 389 (2002).

13

[16]   (a) ADF2013.01. SCM, Theoretical Chemistry, Vrije Universiteit Amsterdam, The Netherlands, http://www.scm.com (2013). (b) C.F. Guerra, J.G. Snijders, G. te Velde, E.J. Baerends. *Theor. Chem. Acc.*, **99**, 391 (1998). (c) G. te Velde, F.M. Bickelhaupt, S.J.A. van Gisbergen, C.F. Guerra, E.J. Baerends, J.G. Snijders, T.J. Ziegler. *Comput. Chem.*, **22**, 931 (2001).

[17]   M. Swart. *Chem. Phys. Lett.*, **580**, 166 (2013).

[18]   S. Grimme, J. Antony, S. Ehrlich, H. Krieg. *J. Chem. Phys.*, **133**, 154104 (2010).

[19]   E. van Lenthe, A. Ehlers, E.-J. Baerends. *J. Chem. Phys.*, **110**, 8943 (1999).

[20]   A. Klamt, G. Schüürmann. *J. Chem. Soc.*, *Perkin Trans., 2*, 799 (1993).

[21]   S.K. Wolff. *Int. J. Quantum Chem.*, **104**, 645 (2005).

[22]   C.C. Pye, T. Ziegler. *Theor. Chem. Acc.*, **101**, 396 (1999).

[23]   M. Swart, E. Rösler, F.M. Bickelhaupt. *Eur. J. Inorg. Chem.*, **2007**, 3646 (2007).

[24]   T.R. Todorović, U. Rychlewska, B. Warzajtis, D.D. Radanović, N.R. Filipović, I.A. Pajić, D.M. Sladić, K.K. Anđelković. *Polyhedron*, **28**, 2397 (2009).

[25]   Z. Kuodis, A. Rutavičius, A. Matijoška, O. Eicher–Lorka. *Cent. Eur. J. Chem.*, **5**, 996 (2007).

[26]   M. Hagar, S.M. Soliman, F. Ibid, S.H. El Ashry. *J. Mol. Struct.*, **1049**, 177 (2013).

[27]   J. Zhang, L. Ma, F. Zhang, Z. Zhang, L. Li, S. Wang. *J. Coord. Chem.*, **65**, 239 (2012).

[28]   H. Keypour, M. Shayesteh, R. Golbedaghi, A. Chehregani, A.G. Blackman. *J. Coord. Chem.*, **65**, 1004 (2012).

[29]   M.A. Carvalho, B.C. Souza, R.E.F. Paiva, F.R.G. Bergamini, A.F. Gomes, F.C. Gozzo, W.R. Lustri, A.L.B. Formiga, G. Rigatto, P.P. Corbi. *J. Coord. Chem.*, **65**, 1700 (2012).

[30]   M. Salehi, R. Kia, A. Khaleghian. *J. Coord. Chem.*, **65**, 3007 (2012).

[31]   L. Ma, J. Zhang, F. Zhang, C. Chen, L. Li, S. Wang, S. Li. *J. Coord. Chem.*, **65**, 3160 (2012).

[32]   M.N. Patel, P.A. Dosi, B.S. Bhatt. *J. Coord. Chem.*, **65**, 3833 (2012).

[33]   F. Fadaee, M. Amirnasr, A. Amirnasr, K. Mereiter, K. Schenk-Joß. *J. Coord. Chem.*, **66**, 1363 (2013).

[34]   D.Y. Ma, L.X. Zhang, X.Y. Rao, T.L. Wu, D.H. Li, X.Q. Xie, H.F. Guo, L. Qin. *J. Coord. Chem.*, **66**, 3261 (2013).

14

Table 1. Crystal data and structure refinement for **1** and **HL·EtOH**.

	1	**HL·EtOH**
Empirical formula	$C_{24}H_{26}Cl_2N_3OPPd$	$C_{26}H_{33}ClN_3O_2P$
Formula weight	580.75	485.97
Temperature/K	296.15	296.15
Crystal system	Triclinic	Triclinic
Space group	*P-1*	*P-1*
a/Å	10.5515(18)	8.9862(6)
b/Å	12.531(2)	10.7502(8)
c/Å	21.514(4)	14.923(1)
α/°	98.909(3)	101.865(1)
β/°	96.810(3)	104.198(1)
γ/°	98.838(3)	97.828(1)
Volume/Å^3	2747.3(8)	1341.0(2)
Z	4	2
ρ_{calc} g/cm^3	1.404	1.204
μ/mm^{-1}	0.948	0.228
F(000)	1176.0	516.0
Crystal size/mm^3	$0.45 \times 0.11 \times 0.042$	$0.1 \times 0.08 \times 0.05$
Radiation	MoKα ($\lambda = 0.71073$)	MoKα ($\lambda = 0.71073$)
2Θ range for data collection/°	1.94 to 43.56	2.906 to 60.116
Reflections collected	22008	21056
Independent reflections	6518 [$R_{int} = 0.0577$]	7796 [$R_{int} = 0.0278$]
Data / restraints / parameters	6518 / 0 / 586	7796 / 0 / 303
Goodness-of-fit on F^2	1.005	1.213
Final R indexes [I>=2σ (I)]	$R_1 = 0.0346$, w$R_2 = 0.0745$	$R_1 = 0.0525$, w$R_2 = 0.1685$
Final R indexes [all data]	$R_1 = 0.0487$, w$R_2 = 0.0792$	$R_1 = 0.0680$, w$R_2 = 0.1790$
Largest ΔF max/min / e Å^{-3}	0.61/-0.39	0.39/-0.28

Table 2. ^{1}H-NMR spectral data (chemical shift (ppm), multiplicity, number of H-atoms, coupling constant J in Hz) of **HL·EtOH** and complexes **1** and **2**.

Assignment	**HL·EtOH** *syn*	**HL·EtOH** *anti*	**1**	**2**
C1	3.30 (s, 9 H)	3.28 (s, 2.7 H)	3.28 (s, 9H)	3.01 (s, 9H)
C2	4.76 (s, 2 H)	4.34 (s, 0.6 H)	4.34 (s, 2H)	3.28 (d, 1H, J = 15 Hz)
C2'				3.58 (d, 1H, J = 15 Hz)
C3	8.79 (d, 1 H, J = 5.0 Hz)	9.02 (d,1H, J = 5.0 Hz)	8.77 (d, 1H, J = 5.0 Hz)	9.39 (s, 1H)
C5	6.83 (m, 1H)	6.86 (m, 0.3 H)	7.48 (dd, 1H, J = 15.0 Hz, J = 10.0 Hz)	7.28 (m, 1H)
C6	7.42 (m, 1 H)	7.42 (0.3 H)	7.72 (t, 1H, J = 8.0 Hz)	7.63 (t, 1 H, J = 5.0 Hz)
C7	7.49 (m, 1 H)	7.49 (m, 0.3 H)	7.85 (t, 1H, J = 7.5 Hz)	7.90 (t, 1H, J = 5.0 Hz)
C8	8.05 (dd, 1 H, J = 5.0 Hz)	7.99 (dd, 0.3 H, J = 5.0 Hz)	8.11 (dd, 1H, J = 10.0 Hz, J = 5.0 Hz)	8.08 (d, 1H, J = 10.0 Hz)
C11	7.19 (m, 4 H)	7.19 (m, 1.2 H)	7.55 (m, 4H)	6.99 (dd, 2H, J = 10.0 Hz, J = 5.0 Hz)
C11'	-	-	-	7.22 (m, 2H)
C12	7.42 (m, 4 H)	7.42 (m, 1.2 H)	7.65 (m, 4H)	7.18 (m, 2H)
C12'	-	-	-	7.37 (m, 2H)
C13	7.42 (m, 2 H)	7.42 (m, 0.6 H)	7.65 (m, 2H)	7.46 (t, 1H, J = 5.0 Hz)
C13'	-	-	-	7.53 (t, 1H, J = 5.0 Hz)
N2	12.10 (s, 1 H)	12.70 (s, 1H)	-	-

Table 3. ^{13}C-NMR spectral data (chemical shift (ppm), coupling constant J in Hz) of **HL·EtOH** and complexes **1** and **2**.

| Assignment	**HL·EtOH** *syn*	**HL·EtOH** *anti*	**1**	**2**
C1	53.4	56.1	53.5	53.4
C2	62.4	63.1	62.4	61.5
C3	143.4 (J = 25.0 Hz)	146.5 (J = 25.0 Hz)	154.0	165.2
C4	135.4 (J = 10 Hz)	135.4 (J = 10 Hz)	135.8 (J = 17.5 Hz)	134.2
C5	133.2	133.3	134.9 (J = 1.25 Hz)	135.4
C6	130.5	130.7	134.3 (J = 7.5 Hz)	134.6
C7	129.4	129.6	134.3 (J = 7.5 Hz)	134.2
C8	126.3 (J = 3.75 Hz)	126.1 (J = 3.75 Hz)	138.1 (J = 10.0 Hz)	138.8
C9	136.5 (J = 18.75 Hz)	136.5 (J = 18.75 Hz)	118.2 (J = 52.5 Hz)	134.6
C10	137.2 (J = 18.75 Hz)	137.2 (J = 18.75 Hz)	127.7 (J = 62.5 Hz)	134.5
C11	133.5 (J = 18.75 Hz)	133.5 (J = 18.75 Hz)	129.4 (J = 12.5 Hz)	133.3
C12	129.1 (J = 7.5 Hz)	129.0 (J = 7.5 Hz)	133.9 (J = 11.25 Hz)	129.6
C12'	-	-	-	129.1
C13	129.4	129.3	132.6 (J = 2.5 Hz)	132.7
C13'	-	-	-	132.1
C14	165.5	160.1	170.0	168.8

17

Table 4. Relevant bond lengths (Å) and angles (°) for **1**, with su's in parentheses.

Bond length	(Å)	Bond length	(Å)
C1-P1	1.822(4)	C25-P2	1.796(4)
C7-P1	1.809(5)	C31-P2	1.792(5)
C13-P1	1.803(5)	C37-P2	1.795(5)
C19-N1	1.290(5)	C43-N4	1.293(5)
C20-N2	1.306(6)	C44-N5	1.311(6)
C20-O1	1.282(5)	C44-O2	1.293(5)
C21-N3	1.507(6)	C45-N6	1.496(5)
C22-N3	1.499(6)	C46-N6	1.501(5)
C23-N3	1.486(6)	C47-N6	1.512(6)
C24-N3	1.486(6)	C48-N6	1.480(6)
N1-N2	1.409(5)	N4-N5	1.410(5)
N1-Pd1	1.980(4)	N4-Pd2	1.974(3)
O1-Pd1	2.073(3)	O2-Pd2	2.066(3)
Cl1-Pd1	2.288(1)	P2-Pd2	2.196(1)
Pd1-P1	2.199(1)	Cl2-Pd2	2.290(1)
Bond angle	(°)	Bond angle	(°)
N1-Pd1-O1	80.2(1)	N1-Pd1-Cl1	175.0(1)
N1-Pd1-P1	95.3(1)	O1-Pd1-Cl1	95.4(1)
O1-Pd1-P1	174.6(1)	Cl1-Pd1-P1	88.92(5)
Pd1-N1-N2	113.6(3)	Pd1-N1-C19	131.6(3)
N1-N2-C20	111.1(4)	C20-O1-Pd1	107.2(3)
C6-C19-N1	129.3(4)	C19-C6-C1	126.5(4)
C6-C1-P1	122.8(3)	C1-P1-Pd1	111.8(1)
C21-C20-O1	117.4(4)	C20-C21-N3	114.2(4)

18

Table 5. The antimicrobial activity of **HL·EtOH** and complexes **1** and **2** (MIC values in μmol L^{-1}).

Microorganisms	HL·EtOH	1	2	K$_2$[PdCl$_4$]	Co(BF$_4$)$_2$·6H$_2$O	Cefotaxime	Amphotericin B
Staphylococcus aureus ATCC 6538	514	430	106	3060	2935	27	-
Pseudomonas aeruginosa ATCC 9027	514	430	212	3060	2935	55	-
Bacillus subtilis ATCC 6633	257	430	106	3060	2935	14	-
Salmonella abony ATCC 6017	257	430	106	3060	2935	55	-
Klebsiella pneumoniae NCIMB 9111	514	430	106	3060	2935	27	-
Escherichia coli ATCC 10536	514	430	212	3060	1467	14	-
Candida albicans ATCC 10231	514	430	212	3060	2935	-	7

19
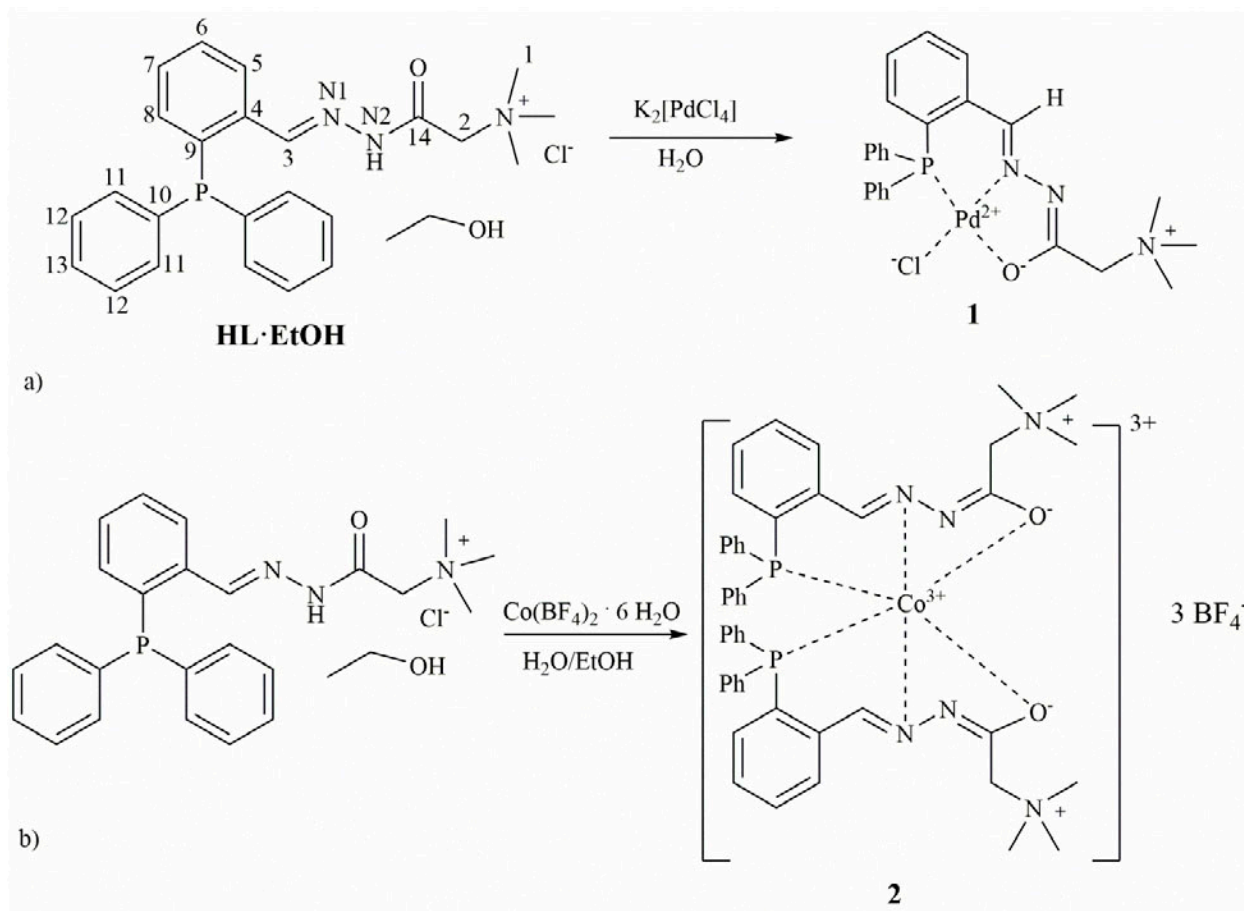
Scheme 1.
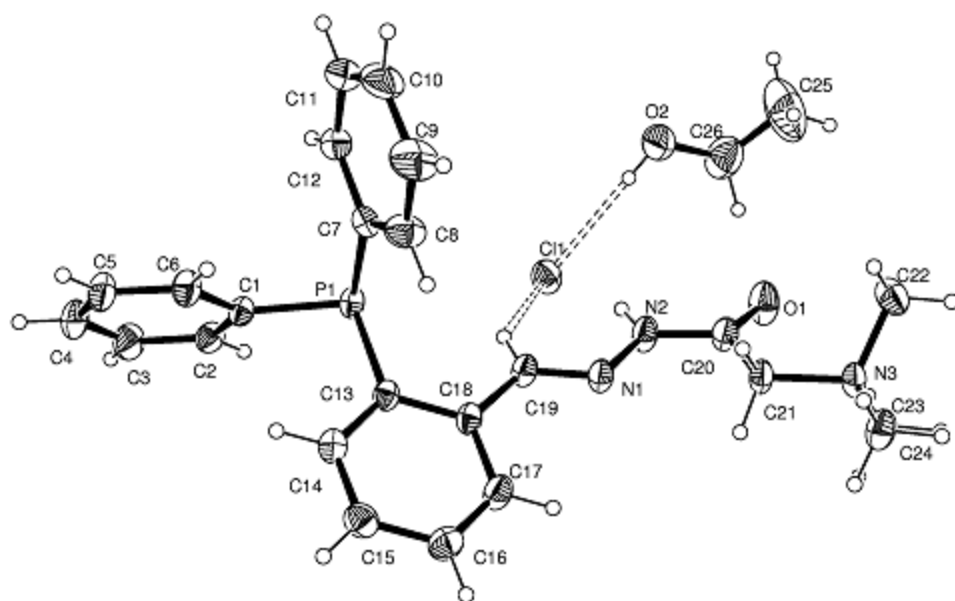
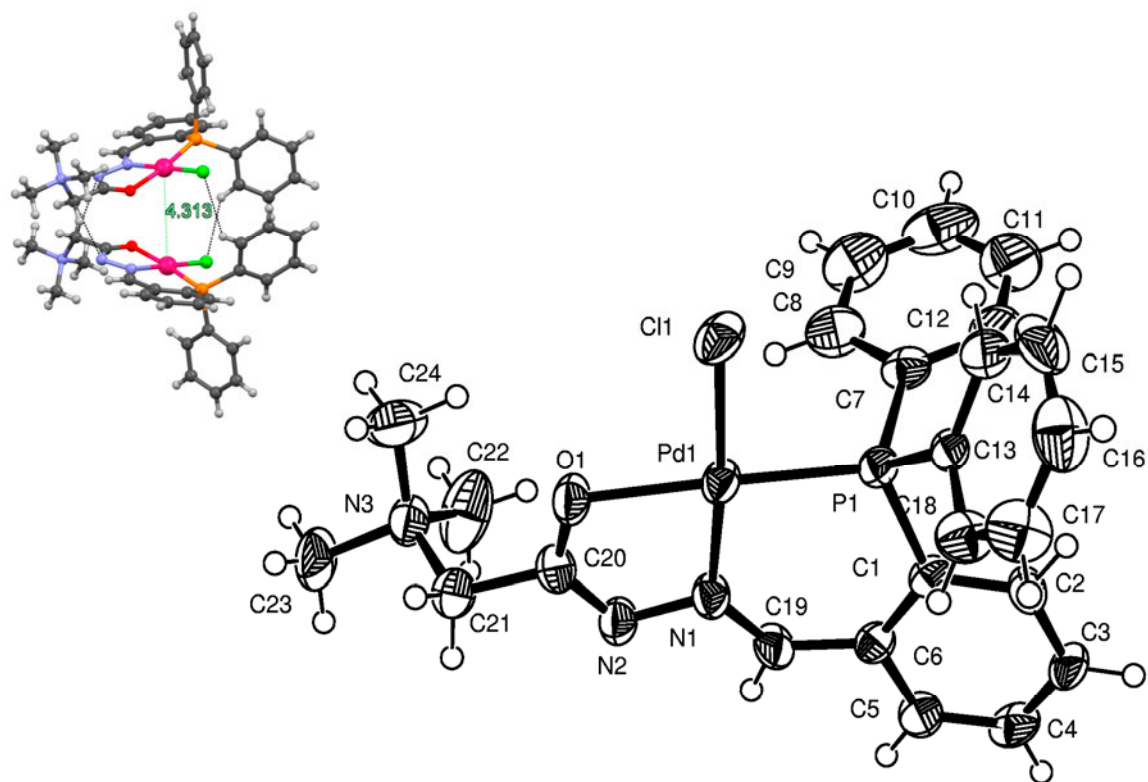Figure 1. Crystal structure of **HL·EtOH**, with thermal ellipsoids at the 50% probability level. Hydrogen bonds are dashed.

Figure 2. Molecular structure of [PdLCl]$^+$ in **1**, with thermal ellipsoids at the 50% probability level. Inset: stacking of two crystallographically independent cations in the crystal structure of **1**.
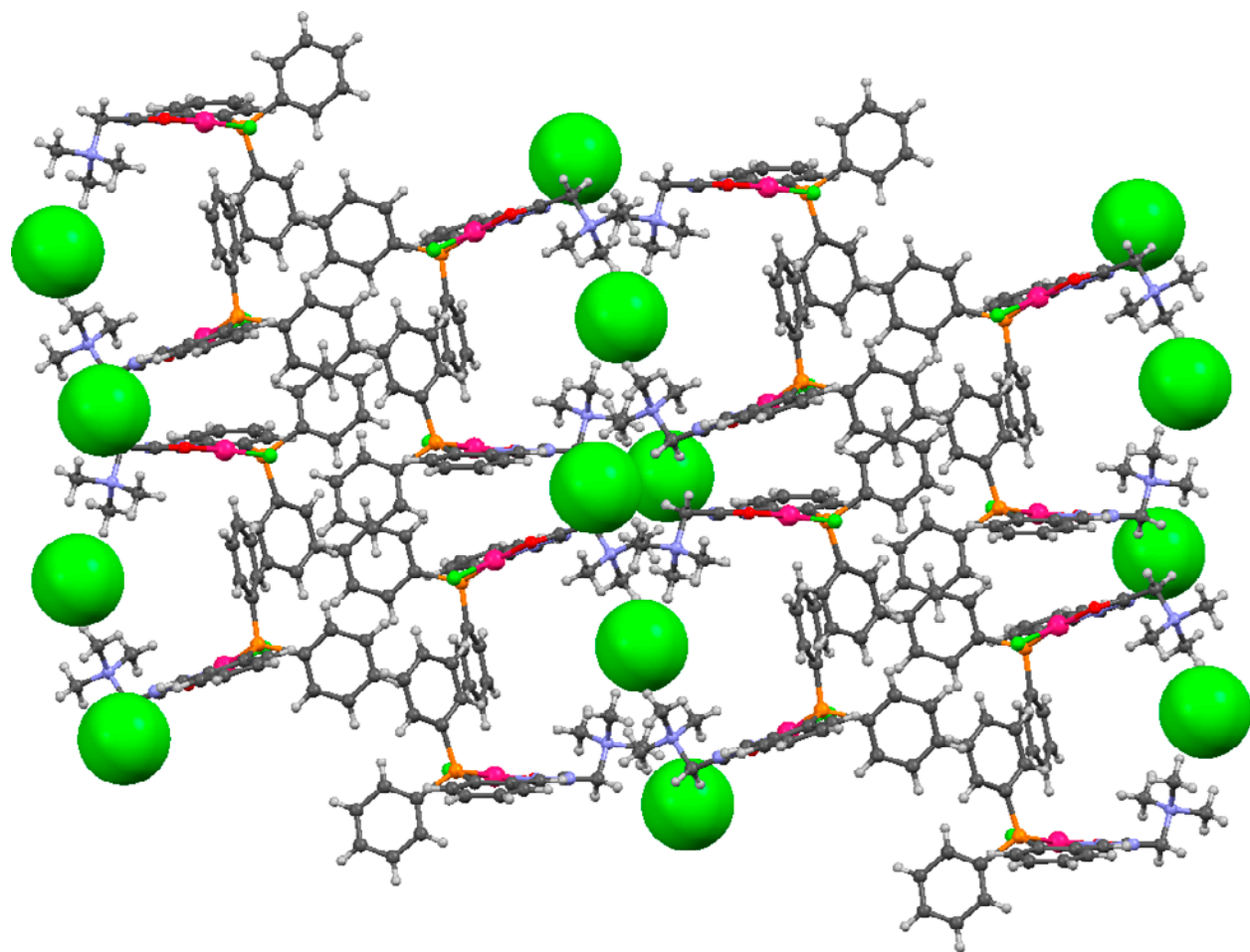
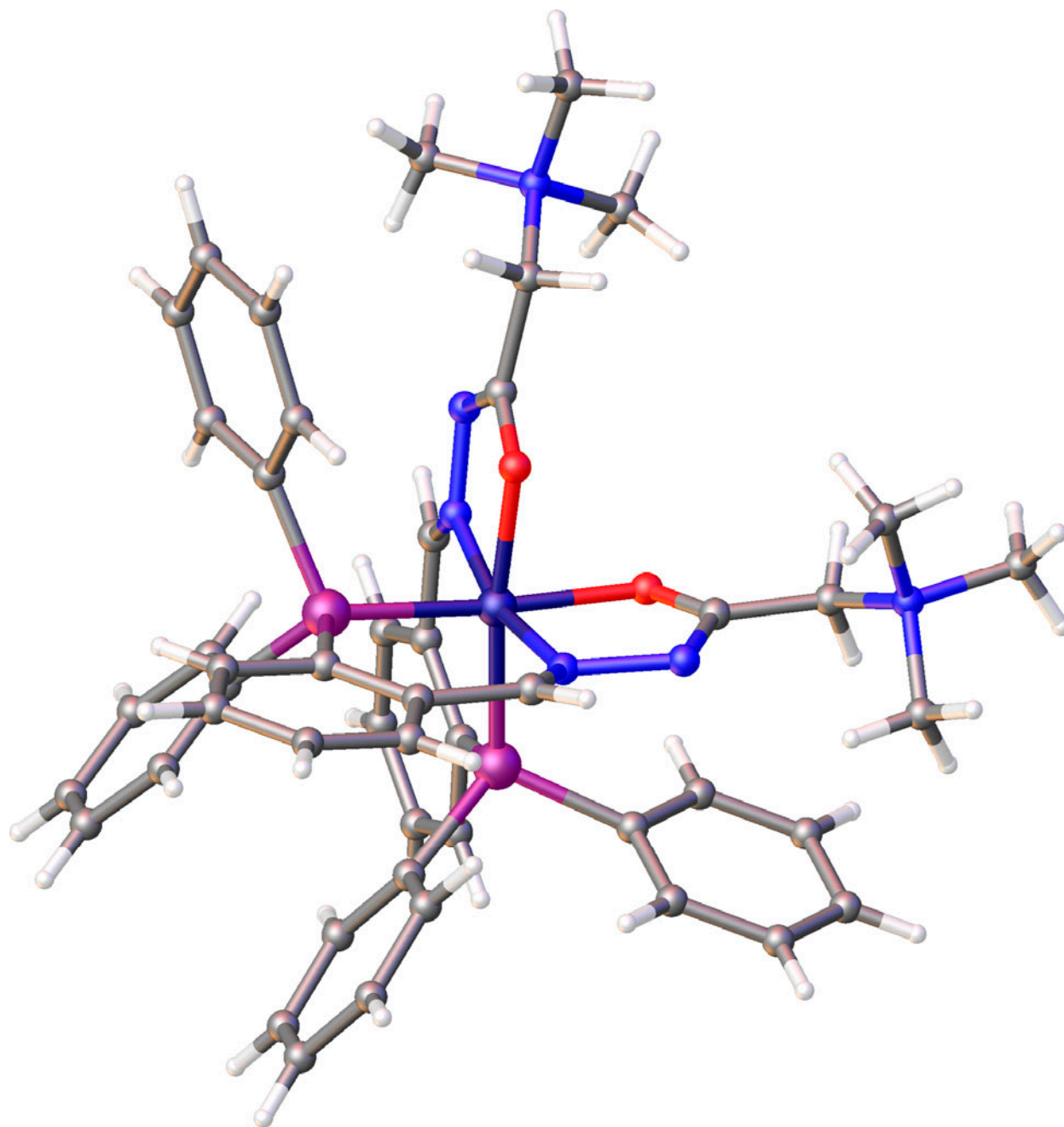Figure 3. Crystal packing of the ordered part of the structure of **1**, showing cations and anions.

23

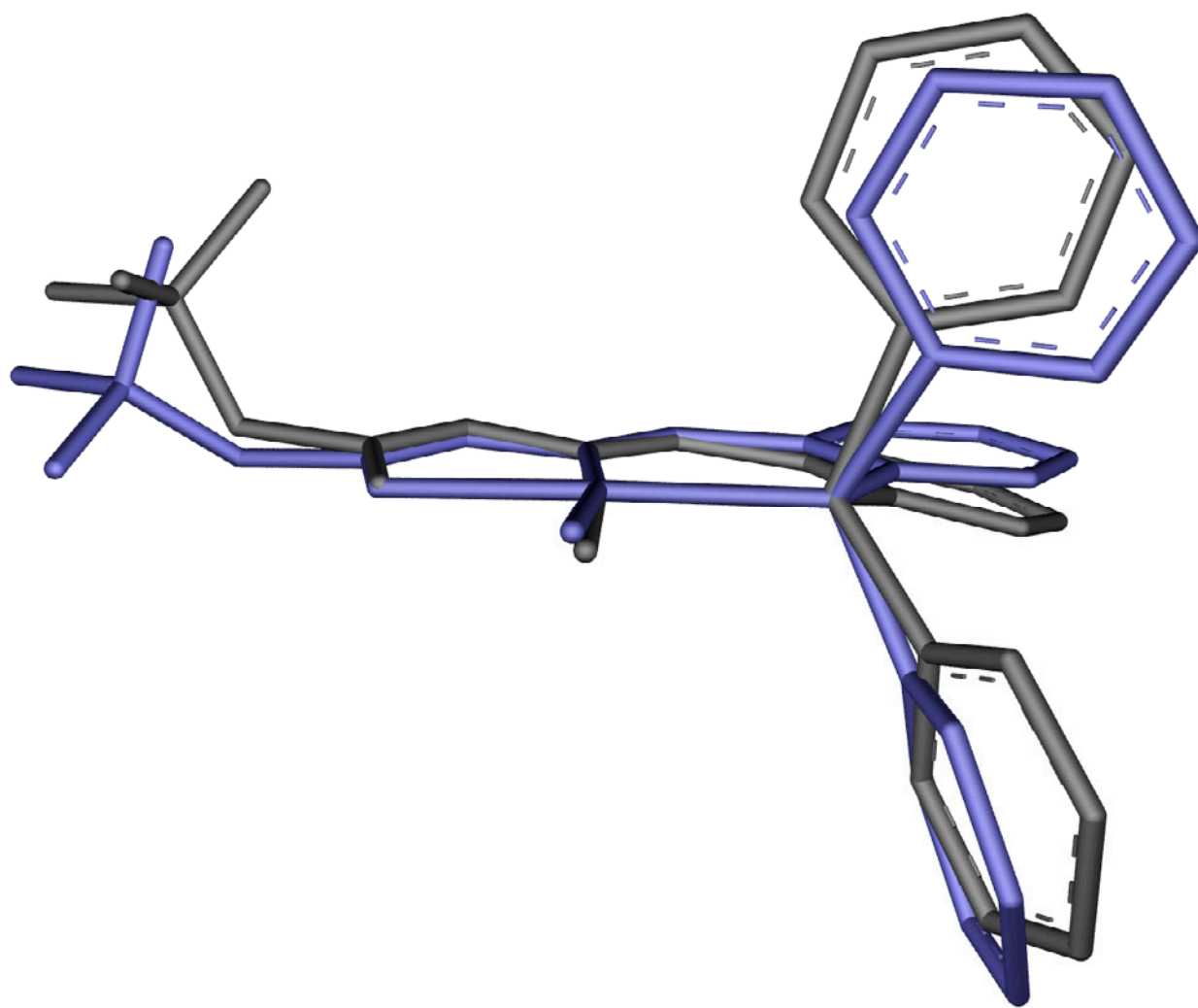Figure 4. Molecular structure of [Co**L**$_2$]$^{3+}$ in **2**, as determined by X-ray diffraction.

Figure 5. Superposition of experimental X-ray (gray) with S12g optimized (light blue) global
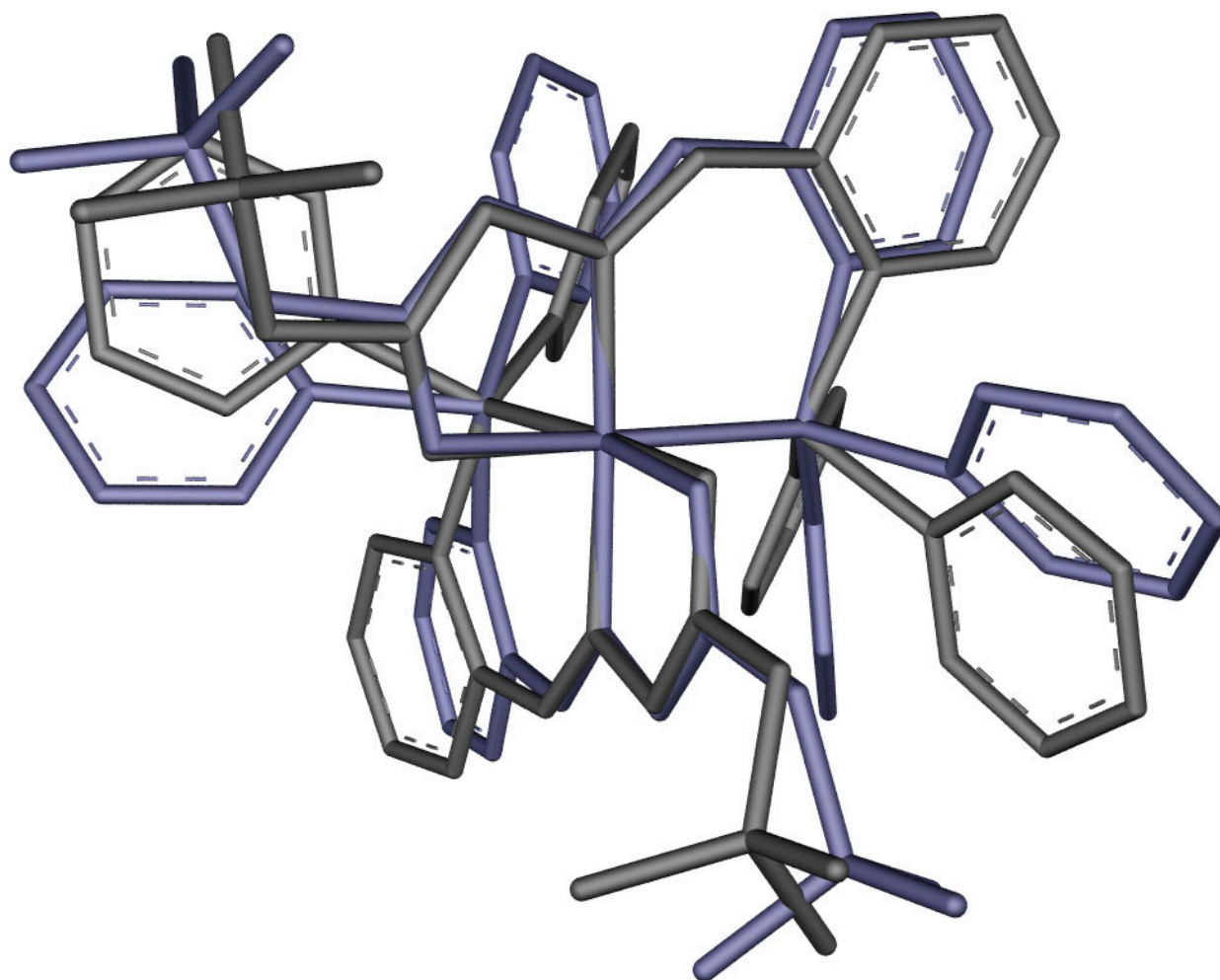minimum structure of [PdLCl]$^+$ cation.
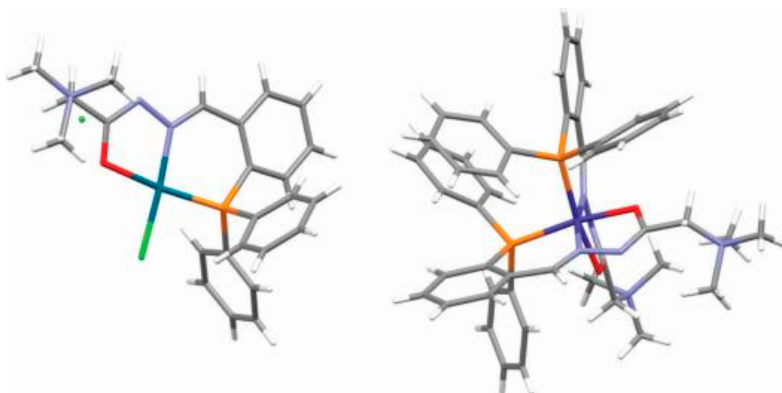
Figure 6. Superposition of experimental X-ray (gray) with S12g optimized (light blue) global minimum structure of $[CoL_2]^{3+}$ cation.

26

27